Journal of Physics: Conference Series **657** (2015) 012008 doi:10.1088/1742-6596/657/1/012008

Nonlinear electromagnetic inverse scattering in via Frozen or Broyden update of the Fréchet derivative

E. Tavanti [1], **C. Estatico** [2], **A. Fedeli** [1], **M. Pastorino** [1], **A. Randazzo** [1]

[1]Department of Electrical, Electronic, Telecommunication Engineering, and Naval Architecture, University of Genoa, Via Opera Pia 11A, I-16145, Genoa, Italy.

[2]Department of Mathematics, University of Genoa, Via Dodecaneso 35, I-16146 Genoa, Italy.

E-mail: emanuele.tavanti@gmail.com

Abstract. Microwave imaging methods are useful for non-destructive inspection of dielectric targets. In this work, a numerical technique for solving the 3D Lippmann-Schwinger integral equation of the inverse scattering problem via Gauss-Newton linearization in Banach spaces is analysed. More specifically, two different approximations of the Fréchet derivative are proposed in order to speed up the computation. Indeed it is well known that the computation of the Fréchet derivative is generally quite expensive in three dimensional restorations. Numerical tests show that the approximations give a faster restoration without loosing accuracy.

1. Introduction

As it is well known the electromagnetic inverse scattering problem is the basic formulation for microwave imaging methods. Although this problem has been suitably studied from a theoretical point of view, new methods are continuously developed to face new and challenging applications. To inspect dielectric targets, several different techniques can be adopted. These techniques has been devised in the last decades starting from some pioneering research results [1],[2]. Some examples can be found in [3]-[12] and in the references therein.

In this context, an approach for solving the Lippmann-Schwinger integral equation of the inverse scattering problem by lossy dielectric targets has been proposed in [13]. It is based on an inexact-Newton method and constituted by two nested loops, and it has been tested versus experimental input data [14]. A review of the obtained results have been reported in [15]. Although such results appear to be quite satisfactory, in particular in dealing with the ill-posedness of the considered inverse problem, one of the main drawback is related to the significant over-smoothing effects associated to the properties of the Hilbert space in which the approach has been developed. In order to mitigate this effect, a new formulation has been proposed in [16], in which the inverse scattering equations have been solved in L^p Banach spaces.

Despite the increasing of the formulation complexity, the new approach has led to a noticeable reduction in the reconstruction errors as compared with solutions developed in the Hilbert spaces. So for, the new approach has been applied to two-dimensional configurations for which a scalar formulation can be used. In the present paper, this method is preliminary extended to treat three-dimensional targets, where the computation of the Fréchet derivative becomes numerically expensive. This way, two different low-cost approximations of the Fréchet derivative, namely the frozen [17] and the Broyden update [18], are investigated in order to obtain a faster reconstruction algorithm.

[1] E-mail: emanuele.tavanti@gmail.com ; alessandro.fedeli@edu.unige.it; matteo.pastorino@unige.it; andrea.randazzo@unige.it.

[2] E-mail: estatico@dima.unige.it. The work of C. Estatico is partly supported by PRIN 2012 N. 2012MTE38N.

2. The 3D microwave inverse scattering model

An unknown dielectric target, located inside an investigation cube V_{inv}, is illuminated by one or more incident known electric fields, generated by proper emitting antennas located outside the cube. For any illumination, at any point $\mathbf{r}$ of the whole three-dimensional space, the electromagnetic interaction between the dielectric object and the incident radiation gives rise to a total electric field $\mathbf{E}_{tot}(\mathbf{r}) = \mathbf{E}_{inc}(\mathbf{r}) + \mathbf{E}_{scatt}(\mathbf{r})$, which is the sum of the incident and the scattered electric fields.

In the inverse scattering model, the measurement of $\mathbf{E}_{tot}(\mathbf{r})$ by several receiving antennas located in a measurement domain V_{obs} external to the investigation cube allows to reconstruct (a suitable approximation of) the unknown dielectric object. In our numerical simulations, the emitting and receiving antennas are uniformly distributed on a fixed sphere enclosing the investigation cube. For sake of simplicity, a single-view case is described in the following. The extension of the mathematical formulation to the multi-view case is however straightforward.

The scattered electric field $\mathbf{E}_{scatt}(\mathbf{r})$ is related to the dielectric properties of the investigated area V_{inv} by means of the following two integral equations, usually referred as data and state equations,

$$\begin{aligned} \mathbf{E}_{scatt}(\mathbf{r}) &= \mathbf{G}_{data}(c\mathbf{E}_{tot})(\mathbf{r}), \qquad \mathbf{r} \in V_{obs} \\ \mathbf{E}_{inc}(\mathbf{r}) &= \mathbf{E}_{tot}(\mathbf{r}) - \mathbf{G}_{state}(c\mathbf{E}_{tot})(\mathbf{r}), \qquad \mathbf{r} \in V_{inv} \end{aligned} \tag{1}$$

where $c(\mathbf{r}) = \epsilon_r(\mathbf{r}) - 1$ is the target contrast function (being ϵ_r the space dependent relative complex dielectric permittivity of the cube V_{inv}), the linear convolution operators $\mathbf{G}_{data}$ and $\mathbf{G}_{state}$ are

$$\begin{aligned} \mathbf{G}_{data}\mathbf{f}(\mathbf{r}) &= -k_0^2 \int_{V_{inv}} \mathbf{f}(\mathbf{r}) \cdot \bar{\mathbf{G}}_0(\mathbf{r}, \mathbf{r}')d\mathbf{r}', \qquad \mathbf{r} \in V_{obs}, \\ \mathbf{G}_{state}\mathbf{f}(\mathbf{r}) &= -k_0^2 \int_{V_{inv}} \mathbf{f}(\mathbf{r}) \cdot \bar{\mathbf{G}}_0(\mathbf{r}, \mathbf{r}')d\mathbf{r}', \qquad \mathbf{r} \in V_{inv}, \end{aligned}$$

being $k_0 = \omega\sqrt{\epsilon_0\mu_0}$ the free-space wavenumber and $\bar{\mathbf{G}}_0(\mathbf{r}, \mathbf{r}') = -\frac{1}{4\pi}\left(\bar{\mathbf{I}} + \frac{\nabla\nabla}{k_0^2}\right)\frac{e^{-jk|\mathbf{r}-\mathbf{r}'|}}{|\mathbf{r}-\mathbf{r}'|}$ is the free-space dyadic Green's function. The data and state equations can be merged in order to obtain the following single non-linear operator equation

$$\mathbf{E}_{scatt}(\mathbf{r}) = \mathbf{G}_{data}\big(\mathbf{C}((\mathbf{I} - \mathbf{G}_{state}\mathbf{C})^{-1}\mathbf{E}_{inc})\big)(\mathbf{r}), \tag{2}$$

where $\mathbf{r} \in V_{obs}$ and $\mathbf{C}$ is the operator such that $\mathbf{C}(\mathbf{f})(\mathbf{r}) = c(\mathbf{r})\mathbf{f}(\mathbf{r})$, $\mathbf{r} \in V_{inv}$. By defining the non-linear operator $\mathbf{F}(c) = \mathbf{G}_{data}\big(\mathbf{C}((\mathbf{I} - \mathbf{G}_{state}\mathbf{C})^{-1}\mathbf{E}_{inc})\big)$ that maps the contrast function c with the scattered electric field $\mathbf{E}_{scatt}$, equation (2) can be written in compact form as follows

$$\mathbf{F}(c)(\mathbf{r}) = \mathbf{E}_{scatt}(\mathbf{r}), \qquad \mathbf{r} \in V_{obs}. \tag{3}$$

The non-linear equation (3) models the full inverse scattering problem: Given the scattered electric field $\mathbf{E}_{scatt}$ (i.e., the data), measured in the measurement domain V_{obs}, find the contrast function c (i.e., the unknown) in the investigation domain V_{inv} such that $\mathbf{F}(c) = \mathbf{E}_{scatt}$.

3. The solution of the inverse problem in Banach spaces via quasi-Newton schemes

By a pure mathematical point of view, the nonlinear operator of (3) is a map $\mathbf{F}: C \to E$ between a linear functional space C of the contrast functions and the functional space E of the electric fields. In the classical solving schemes, C and E are $L^\infty(V_{inv}) \subset L^2(V_{inv})$ and $L^2(V_{obs})$ respectively, being L^2 the Hilbert spaces of square-integrable functions. In our solving scheme, C and E are the more general Banach spaces $L^\infty(V_{inv}) \subset L^p(V_{inv})$ and $L^p(V_{obs})$ of p-integrable functions, with $1 < p < 2$, so that the more recent theory of regularization in Banach spaces can be applied [19]-[21]. Indeed, it has been shown that the resolution of functional equations in L^p Banach spaces, with $1 \leq p < 2$, reduces over-smoothness effects of the classical L^2 solutions, leading to a better localization of the discontinuities of the scatterers.

To solve (3), a Newton-like iterative method is applied to minimize the $L^p(V_{obs})$ residual functional

$\Omega_p: L^p(V_{inv}) \to \mathbb{R}$ defined as follows

$$\Omega_p(c) = \frac{1}{p}\|\mathbf{F}(c) - \mathbf{E}_{scatt}\|^p_{L^p(V_{obs})}\,.$$

In particular, any linearized equation of the Newton scheme is solved by means of a gradient-like iterative regularization method for inverse problems in Banach spaces [19]. In our three-dimensional case, the Fréchet derivative $\mathbf{F}'_c$: $L^p(V_{inv}) \to L^p(V_{obs})$ of the operator $\mathbf{F}$ at point c is given by

$$\mathbf{F}'_c\delta(\mathbf{r}) = \mathbf{G}^c_{data}(\delta\mathbf{E}^c_{tot})(\mathbf{r}),\ \mathbf{r} \in V_{obs},\quad \forall\delta \in L^p(V_{inv})\,, \tag{4}$$

where $\mathbf{E}^c_{tot}(\mathbf{r}) = ((\mathbf{I} - \mathbf{G}_{state}\mathbf{C})^{-1}\mathbf{E}_{inc})(\mathbf{r})$, $\mathbf{r} \in V_{inv}$, and the operator $\mathbf{G}^c_{data}$ is given by

$$\mathbf{G}^c_{data}\mathbf{f}(\mathbf{r}) = -k_0^2 \int_{V_{inv}} \mathbf{f}(\mathbf{r}) \cdot \overline{\mathbf{G}}_c(\mathbf{r}, \mathbf{r}')d\mathbf{r}'\,, \mathbf{r} \in V_{obs}, \tag{5}$$

being $\overline{\mathbf{G}}_c$ the dyadic Green's function for an inhomogeneous background characterized by c [22].

As it is well-known, together to convergence issues, the drawback of Newton methods in real applications is the generally expensive computation of the new Fréchet derivative at each iteration. On the other hand, it is expected that the "new" Fréchet derivative at iteration k could be suitably approximated by means of the "previous" one at iteration $k-1$. Basically, this is the key point of several generalizations named as *quasi-Newton* methods. In this paper we deal with the frozen-Newton method [17] and the Broyden-Newton method [18], as summarized in the following steps.

I) Let $c_0 \in L^\infty(V_{inv})$ be an initial guess (the null function c_0 is often used in the applications), and comupute the Fréchet derivative of $\mathbf{F}$ at point c_0, denoted as $\mathbf{F}'_0$. Set $n := 0$ (please notice that n denotes the outer interation index).

II) Frozen update: if $n \bmod s = 0$ then $\tilde{\mathbf{F}}'_n = \mathbf{F}'_n$, that is, let $\tilde{\mathbf{F}}'_n$ be the (new) Fréchet derivative $\mathbf{F}'_n$ of $\mathbf{F}$ at point c_n; else set $\tilde{\mathbf{F}}'_n = \tilde{\mathbf{F}}'_{n-1}$, (i.e., use the same derivative of the previous step)
Broyden update: if $n \bmod s = 0$ then $\tilde{\mathbf{F}}'_n = \mathbf{F}'_n$, else let $\tilde{\mathbf{F}}'_n$ be the approximation of the Fréchet derivative $\mathbf{F}'_n$ of $\mathbf{F}$ at point c_n defined by the following Broyden update

$$\tilde{\mathbf{F}}'_n = \tilde{\mathbf{F}}'_{n-1} + \frac{(\mathbf{F}(\mathrm{c}_n) - \mathbf{F}(c_{n-1})) - \tilde{\mathbf{F}}'_{n-1}\delta_{n-1}}{\|\delta_{n-1}\|^2_{L^2(V_{inv})}}\delta^T_{n-1}.$$

III) Compute a regularized solution of the linear system in $L^p(V_{inv})$ with respect to the unknown function δ_n

$$\tilde{\mathbf{F}}'_n\delta_n = \mathbf{E}_{scatt} - \mathbf{F}(c_n) \tag{6}$$

by means of the minimization of the functional $\frac{1}{p}\left\|\tilde{\mathbf{F}}'_n\delta_n - \left(\mathbf{E}_{scatt} - \mathbf{F}(c_n)\right)\right\|^p_{L^p(V_{obs})}$ in $L^p(V_{inv})$ Banach space, for $1 < p < 2$. To this end, we consider an early stop of the following Landweber iterative method for linear equations in $L^p(V_{inv})$ [23].
Let $\delta^*_{n,0} = 0 \in L^q(V_{inv})$ be the inner initial guess. Then for $k = 0,1,2,\ldots$ (please notice that k denotes the inner interation index), compute the iterative steps

$$\delta^*_{n,k+1} = \delta^*_{n,k} - \tau_k\tilde{\mathbf{F}}'^*_n\mathbf{J}_p\left(\tilde{\mathbf{F}}'_n\delta_{n,k} - \left(\mathbf{E}_{scatt} - \mathbf{F}(c_n)\right)\right), \tag{7}$$

$$\delta_{n,k+1} = \mathbf{J}_q\left(\delta^*_{n,k+1}\right), \tag{8}$$

where q is the Hölder conjugate of p, that is, $\frac{1}{p} + \frac{1}{q^*} = 1$, until a stopping rule is satisfied (e.g., a maximum number of inner iterations k_{max} is reached or the norm of the functional to be minimized falls below a fixed threshold). Here $\tau_k > 0$ is the suitable step size, $\mathbf{J}_p$: $L^p(V_{obs}) \to L^q(V_{obs})$ and $\mathbf{J}_q$: $L^q(V_{inv}) \to L^p(V_{inv})$ denote the normalized duality maps between Banach spaces defined as

$\mathbf{J}_s(v) = \partial\left(\frac{1}{r}\|v\|_{L^s}^2\right) = \|v\|_{L^s}^{2-s}|v|^{s-1}e^{j\arg(v)}$, if $v \neq 0$, and $\mathbf{J}_s(0) = 0$, for any $s > 1$ [20]. Set $\delta_n := \delta_{n,k_{max}}$.

IV) Update the current quasi-Newton solution by setting $c_{n+1} = c_n + \delta_n$ and let $n := n + 1$. Stop if a predefined stopping rule (e.g., the discrepancy principle $\Omega_p(c_n) < p\epsilon^p$, being ϵ an estimate of the $L^p(V_{obs})$-norm of the noise on $\mathbf{E}_{scatt}$) is satisfied elsewhere go to step II.

A. The Frozen and the Broyden updates

In the frozen method, the same Fréchet derivative computed at iteration k is used (i.e, is "frozen") for a fixed number s of subsequent iterations $k+1, \dots, k+s-1$ [17].

In the Broyden method, a special low-cost (i.e., rank-1) update of the Fréchet derivative is computed at each iteration [18], as now sketched. Differing from the straightforward one dimensional case, the difference $\mathbf{F}(c_n) - \mathbf{F}(c_{n-1}) \in L^p(V_{obs})$ does not give us enough information to approximate the whole linear operator $\mathbf{F}'_{\mathrm{c_n}}$. On the other hand, the difference $\mathbf{F}(c_n) - \mathbf{F}(c_{n-1})$ gives us information about the directional derivative of $\mathbf{F}$ on the direction $\delta_{n-1} = c_n - c_{n-1}$, since $\mathbf{F}'_{\mathrm{c_n}}\delta_{n-1} = \mathbf{F}(c_n) - \mathbf{F}(c_{n-1}) + O(\|\delta_{n-1}\|^2)$. On this ground, the Broyden update modifies the Fréchet derivative along the direction $\delta_{n-1} = c_n - c_{n-1}$ only, by means of the increment $\mathbf{F}(c_n) - \mathbf{F}(c_{n-1})$, leaving unchanged the operator on the subspace orthogonal to δ_{n-1}. With standard Hilbertian decomposition $v = \alpha\delta_{n-1} + u$, where $u \perp v$, $\alpha = \frac{\delta_{n-1}^T}{\|\delta_{n-1}\|^2}v$ and $\|u\| = 1$, we have that

$$\mathbf{F}'_{\mathrm{c_n}}v = \mathbf{F}'_{\mathrm{c_n}}(\alpha\delta_{n-1} + u) = \alpha\mathbf{F}'_{\mathrm{c_n}}\delta_{n-1} + \mathbf{F}'_{\mathrm{c_n}}u = \alpha\mathbf{F}'_{\mathrm{c_n}}\delta_{n-1} - \alpha\mathbf{F}'_{\mathrm{c_{n-1}}}\delta_{n-1} + \alpha\mathbf{F}'_{\mathrm{c_{n-1}}}\delta_{n-1} + \mathbf{F}'_{\mathrm{c_n}}u \approx$$
$$\alpha\mathbf{F}'_{\mathrm{c_n}}\delta_{n-1} - \alpha\mathbf{F}'_{\mathrm{c_{n-1}}}\delta_{n-1} + \alpha\mathbf{F}'_{\mathrm{c_{n-1}}}\delta_{n-1} + \mathbf{F}'_{\mathrm{c_{n-1}}}u = \alpha\big(\mathbf{F}(\mathrm{c_n}) - \mathbf{F}(\mathrm{c_{n-1}})\big) - \alpha\mathbf{F}'_{\mathrm{c_{n-1}}}\delta_{n-1} +$$
$$\mathbf{F}'_{\mathrm{c_{n-1}}}v = \mathbf{F}'_{\mathrm{c_{n-1}}}v + \left[\frac{1}{\|\delta_{n-1}\|^2}\big(\mathbf{F}(\mathrm{c_n}) - \mathbf{F}(\mathrm{c_{n-1}}) - \mathbf{F}'_{\mathrm{c_{n-1}}}\delta_{n-1}\big)\delta_{n-1}^T\right]v,$$

that is,

$$\mathbf{F}'_{\mathrm{c_n}} \approx \mathbf{F}'_{\mathrm{c_{n-1}}} + \frac{\mathbf{F}(\mathrm{c_n}) - \mathbf{F}(\mathrm{c_{n-1}}) - \mathbf{F}'_{\mathrm{c_{n-1}}}\delta_{n-1}}{\|\delta_{n-1}\|^2}\delta_{n-1}^T .$$

4. A numerical validation

The data and state scattering equations (1) are discretized by using pulse basis functions and Dirac's delta weighting functions [24]. In particular, the investigation domain V_{inv} is discretized into N cubic voxels of centers $\mathbf{r}_n^{inv}$, $n = 1, \dots, N$, and the observation domain is composed by M measurement points located at positions $\mathbf{r}_m^{meas}$, $m = 1, \dots, M$. We focus on the investigation domain shown in Figure 1; it contains a cube and a parallelepiped of equal relative dielectric permittivity and it is partitioned with $N = 10648$. The measurement points are $M = 50$, uniformly located on a sphere of radius $2\,m$ and centered in $(0; 0; 0)$. Six views are used, with plane waves at $300\,MHz$ as illuminating sources. It is worth noting that, in the numerical implementation of the approach, a BiCGStab-FFT algorithm [24] has been used to speed up the computation of the total internal field and of the inhomogeneous dyadic Green's function [22]. To achieve a comparison, we use $p \in \{1.2, 1.3, \dots, 2.2\}$ inside the previously introduced updating methods for Fréchet derivatives, with $s = 4$, and the complete one. We set maximum numbers of outer and inner iterations equal to 20 and 10, respectively, without stopping thresholds.

The following errors are used to quantify the reconstruction quality of the objects and background

$$E_{obj} = \frac{1}{N_{obj}}\sum_{\mathbf{r}_i^{inv} \in V_{obj}} \frac{\left|\hat{c}\left(\mathbf{r}_i^{inv}\right) - c\left(\mathbf{r}_i^{inv}\right)\right|}{\left|c\left(\mathbf{r}_i^{inv}\right) + 1\right|} \quad E_b = \frac{1}{N_b}\sum_{\mathbf{r}_i^{inv} \in V_b} \frac{\left|\hat{c}\left(\mathbf{r}_i^{inv}\right) - c\left(\mathbf{r}_i^{inv}\right)\right|}{\left|c\left(\mathbf{r}_i^{inv}\right) + 1\right|}.$$

where V_{obj} is objects' domain (N_{obj} voxels), V_b is background's one (N_b) and $\hat{c}\left(\mathbf{r}_i^{inv}\right)$ are contrast function's reconstructed values. Table 1 summarizes the results.

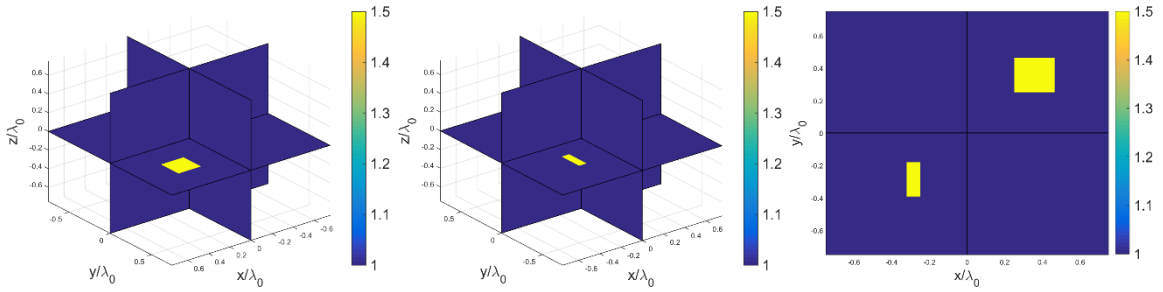

Figure 1. Actual distribution of the relative dielectric permittivity. Three-dimensional views (with slices along the planes $x = 0$, $y = 0$ and $z = 0$) and two-dimensional cut on the x-y plane.

p	Frozen			Broyden			Complete		
	E_{obj}	E_b	Time [s]	E_{obj}	E_b	Time [s]	E_{obj}	E_b	Time [s]
1.2	0.20	1.5 10^{-3}	531	0.23	0.9 10^{-3}	427	0.20	1.6 10^{-3}	2816
1.4	0.25	2.6 10^{-3}	366	0.27	3 10^{-3}	378	0.25	2.6 10^{-3}	1820
1.6	0.27	3.4 10^{-3}	359	0.29	3.6 10^{-3}	373	0.27	3.4 10^{-3}	1794
1.8	0.29	4.2 10^{-3}	366	0.29	4.4 10^{-3}	369	0.29	4.2 10^{-3}	1800
2.0	0.29	4.8 10^{-3}	357	0.30	4.8 10^{-3}	372	0.29	4.8 10^{-3}	1790
2.2	0.30	5.4 10^{-3}	390	0.30	5 10^{-3}	385	0.30	5.4 10^{-3}	1821

Table 1. Errors and computational times upon p.

We see that as p approaches to 2.0 or higher values, both E_{obj} and E_b grow; this supports a choice of $1 < p < 2$ when we are interested in detection of relatively small discontinuities like those in our investigation domain. Figures 2-3 report the reconstructed dielectric scenes. Concerning the approximations of Fréchet derivatives, we note that both Broyden and frozen strategies drastically reduce the computational time by keeping errors very close to the exact derivative case.

5. Conclusions

In this paper, an approach for solving microwave imaging of lossy dielectric targets, which was originally developed for treating two-dimensional configurations, has been extended to inspecting three-dimensional targets. The approach is based on the vector integral equations of the inverse scattering problem (Green's tensor formulation) and on the application of an inexact-Newton method developed in L^p Banach spaces with approximation of the Fréchet derivatives. Some preliminary numerical results have been reported. Further activity will be devoted to inspecting more complex targets and to define rules for a proper choice of the optimum p-parameter, which is of course application-dependent, even by using real experimental data.

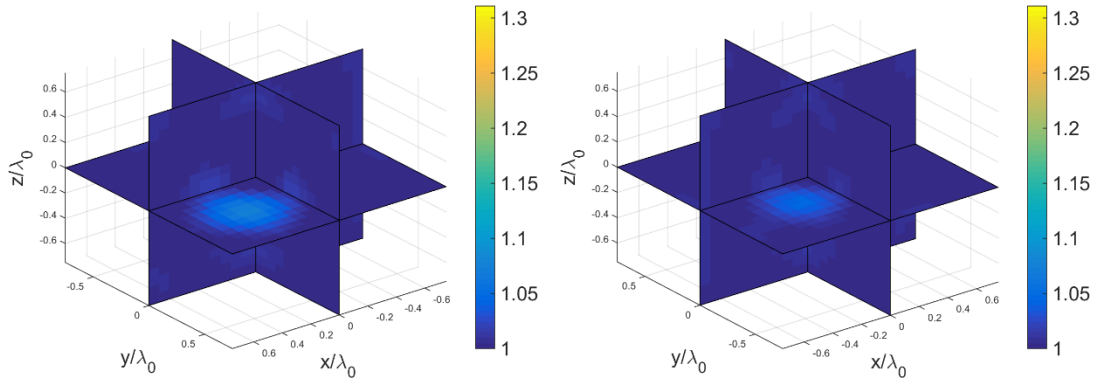

Figure 2. Three-dimensional views (with slices along the planes $x = 0$, $y = 0$ and $z = 0$) of the reconstruction distributions of the relative dielectric permittivity (exact Fréchet derivative, $p = 2.0$).

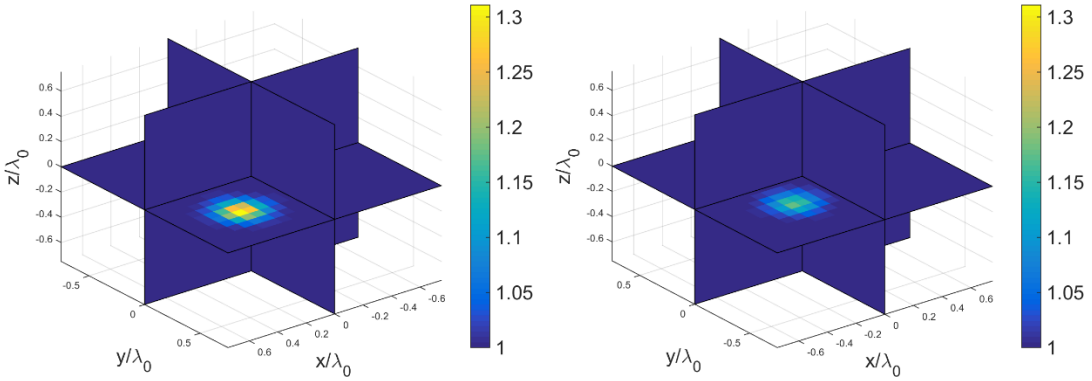

Figure 3. Three-dimensional views (with slices along the planes $x = 0$, $y = 0$ and $z = 0$) of the reconstruction distributions of the relative dielectric permittivity (exact Fréchet derivative, $p = 1.2$).

References

[1] Bolomey J C, Lesselier D, Pichot C and Tabbara W 1981 *IEEE Trans. Antennas Propagat*. **29** 206-212.
[2] Bolomey J C, Izadnegahdar A, Jofre L, Pichot C, Peronnet G and Solaimani M 1982 *IEEE Trans. Microwave Theory Tech*. **30** 1998-2000.
[3] Lesselier D and Bowler J 2002 Special issue on electromagnetic and ultrasonic nondestructive evaluation *Inv. Probl.* **18**.
[4] Chen C C, Johnson J T, Sato M and Yarovoy A G 2007 Special issue on subsurface sensing using ground-penetrating radar *IEEE Trans. Geosci. Remote Sens*. **45**.
[5] Zhang Z Q and Liu Q H 2004 *IEEE Trans. Biomed. Eng*. **51** 544-548.
[6] Gdoura S and Lesselier D 2012 *Proc. 2nd Int. Workshop on New Comput. Meth. for Inv.Probl.*
[7] van den Berg P M and Kleinman R E 1997 *Inv. Probl*. **13**. 1607-1620.
[8] Abubakar A, van den Berg P M and Mallorqui J J 2001 *IEEE Trans. Microwave Theory Tech*. **50** 1761-1771.
[9] De Zaeytijd J, Franchois A, Eyraud C and Geffrin J-M *IEEE Trans. Antennas Propagat*. **55** 3279-3292.
[10] Rubæk T, Meaney P M, Meincke P and Paulsen K D 2007 *IEEE Trans. Antennas Propagat*. **55** 2320-2331.
[11] Lambert M and Lesselier D 2000 *Inv. Probl*. **16** 563-576.
[12] Kooij B J, Lambert M and Lesselier D 1999 *Radio Sci.* **34** 1361-1371.
[13] Estatico C, Pastorino M and Randazzo A 2005 *IEEE Trans. Geosci Remote Sens*. **43** 2593-2505.
[14] Estatico C, Bozza G, Massa A, Pastorino M and Randazzo A 2005 *Inv. Probl.* **21** S81-94.
[15] Pastorino M 2010 *Microwave Imaging* (Hoboken: John Wiley & Sons).
[16] Estatico C, Pastorino M and Randazzo A 2012 *IEEE Trans. Antennas Propagat*. **60** 3373-3381.
[17] Jin Q 2010 *Mathematics of Computation* **79** 2191-2211.
[18] Broyden C G 1965 *Mathematics of Computation* **19** 577-593.
[19] Daubechies I, Defrise M and De Mol C 2004 *Comm. on Pure and Applied Math*. **57** 1413-1457.
[20] Schuster T, Kaltenbacher B, Hofmann B, and Kazimierski K S, 2010 *Regularization methods in Banach spaces*. Radon Series on Computational and Applied Mathematics.
[21] Hein T and Kazimierski K S 2010 *Inv. Probl*. **26** 055002.
[22] Livesay D E and Chen K M 1974 *IEEE Trans. Microwave Theory Tech*. **MTT-22** 1273-1280.
[23] Schöpfer F, Louis A K, and Schuster T, 2006 *Inv. Probl.* **22** 311-329.
[24] Xu X, Liu Q H and Zhang Z Q 2002 *Proc. IEEE Int. Symp. Antennas and Prop. Soc.* **2** 614-617.